Multiple Atlases-Based Joint Labeling of Human Cortical Sulcal Curves

Ilwoo Lyu[1], Gang Li[2], Minjeong Kim[2], and Dinggang Shen[2]

[1] Department of Computer Science, University of North Carolina, Chapel Hill, NC 27599, USA
ilwoolyu@cs.unc.edu
[2] Department of Radiology and BRIC, University of North Carolina, Chapel Hill, NC 27599, USA
{gang_li,mjkim,dgshen}@med.unc.edu

Abstract. We present a spectral-based sulcal curve labeling method by considering geometrical information of neighboring curves in a multiple atlases-based framework. Compared to the conventional method, we propose to use neighboring curves for avoiding ambiguity in curve-by-curve labeling and to integrate the labeling results obtained from multiple atlases for consistent labeling. In particular, we compute a histogram of points on the neighboring curves as a new feature descriptor for each point on a sulcal curve under consideration. To better resolve ambiguity in the curve labeling, we also employ the neighboring curves that are parallel to major sulcal curves. Moreover, we further integrate all the results from multiple atlases into a linear system, by solving which our method ultimately gives accurate labels to the major curves in the subjects. Experimental results on evaluation of 12 major sulcal curves of 12 human cortical surfaces indicate that our method achieves higher labeling accuracy 7.87% compared to the conventional method, while reducing 4.41% of false positive labeling errors on average.

Keywords: sulcal curve labeling, multiple atlases, spectral matching.

1 Introduction

The sulcal folding patterns of human cortical fundic regions are used as key features for analyzing brain function, monitoring brain growth, and discovering diseases. Since sulcal curves can be defined along fundic regions, automatic labeling of sulcal curves is important for these studies. There have been recent studies on automatic extraction of sulcal curves on human cortical surfaces [1,2]. However, these methods extract not only major curves but also many extraneous minor curves, which should be further removed for sulcal curve labeling. Due to the extremely complicated and variable sulcal folding patterns and extraneous minor sulcal branches, even if sulcal curves can be perfectly extracted, it is still challenging to identify major curves among the automatically extracted ones.

Atlas(es)-based sulcal curve labeling methods have been proposed for automatic labeling of major curves [3,4,5]. Compared to the single atlas-based methods [3,4], the multiple atlases-based labeling method is thought to be able to

B.H. Menze et al. (Eds.): MCV 2012, LNCS 7766, pp. 124–132, 2013.

give more accurate labels by considering individual sulcal variability. Recently, a spectral-based sulcal curve labeling method using multiple atlases has been reported [5]. In their method, they just picked the most matched sulcal curve from the multiple atlases to label the corresponding curve in the subject. The correspondence is established by solving an affinity matrix that stores all possible assignments based on the geometric features between two curves under consideration. However, there are two main drawbacks in their method. First, since only the best matched curve is considered as the candidate to label the subject, large false positive errors can be introduced if there is no similar curve in the atlases or the number of atlases is too small. Second, the labeling process is done independently for each major curve without considering its neighboring curves. This could reduce a chance for the major curves to be accurately labeled due to the ambiguity in the curve matching.

In this paper, we present a sulcal curve labeling method for cortical surfaces, which jointly exploits the geometric information of multiple atlases and neighboring curves in the subject space. We focus on "finding correct assignments", which can be formulated as a linear system similarly as in [6]. Specifically, for the feature description, each curve stores its neighboring curves' information (i.e., a histogram of position information of points on the neighboring curves), and in the curve matching, a major curve finds the most similar curves in the subject, guided by its neighboring curves. In addition, we incorporate all labeling results obtained from multiple atlases since it is likely that major curves in the atlases are only partially similar to those in the subject. To this end, we extend the affinity matrix in [6] to integrate labeling results into a linear system. Experimental results indicate that our method achieves 7.87% improvement of labeling accuracy as well as 4.41% reduction of false positive labeling errors on average for 12 major curves on 12 cortical surfaces, compared to the conventional method [5].

2 Method

Given a set of sulcal curves P in atlases and that of unlabeled sulcal curves Q in the subject, our goal is to label major curves in Q while discarding minor ones in Q. Note that the curves in P are pre-labeled major curves by following neuroanatomical conventions while Q contains (possibly disconnected) major curves and many minor ones. For curve labeling, we first automatically extract sulcal curves from the triangulated cortical surface using [1] and deform all curves in each atlas to the subject space using a diffeomporphic surface registration method [7]. It is worth noting that landmark-free surface registration methods can only roughly align the sulcal folding patterns [8], thus still leaving a certain amount of ambiguity in the curve labeling (see Fig. 1a). To better resolve ambiguity in the labeling, unlike the "hard" matching strategy in the conventional method, we use the geometric features of the major curve and its nearby curves for measuring curve similarity. Moreover, the final label is jointly determined by all atlases, which differs from the conventional method that directly retrieves the label from the most similar curve in a selected atlas.

2.1 Spectral-Based Curve Matching Using Neighboring Curves

To measure similarity for every possible pair of curves $p \subseteq P$ and $q \subseteq Q$, we basically measure the individual and pairwise affinities of an assignment $a = (p_i, q_j)$, where $p_i \in p$ and $q_j \in q$. For an assignment a, we denote $D(a)$ as the displacement vector between geometric features of p_i and q_j, each element of which is normalized with respect to its maximum value. Let w be a nonnegative weight vector that gives the importance of every element in $D(a)$. The individual affinity is then defined as follows:

$$A(a) = \exp(-\frac{\|D(a)\|_w^2}{2\sigma^2}) \ , \tag{1}$$

where $\|D\|_w$ denotes the weighted L_2-norm of D with respect to the weight vector w and σ is a user-provided regularization parameter. Similarly, for two distinct assignments a and b, the pairwise affinity is given by

$$A(a, b) = \exp(-\frac{\|D(a, b)\|_w^2}{2\sigma^2}) \ , \tag{2}$$

where $D(a, b) = D(a) - D(b)$.

Geometric Features Considering Neighboring Curves. Several geometric features are defined for each sulcal point, i.e., positions, curvatures, and unit tangent vectors from the major curve under consideration. Besides, we further incorporate the features from its neighboring curves. Basically, we calculate a histogram based on the position information of the neighboring curves in the Euclidean space. Given a major curve $p = \{p_1, \cdots, p_i, \cdots, p_N\}$ with N sulcal points for $p \subseteq P$, let S_p be a set of its neighboring curves. To compute a histogram of the neighboring sulcal points around a point $p_i \in p$, we first build a spherical kernel K centered at p_i with radius r. The size of r is automatically determined by the maximum Hausdorff distance between p and s for $\forall s \subseteq S_p$.

$$r = \max_{s \subseteq S_p} d_H(p, s) \ , \tag{3}$$

where $d_H(\cdot, \cdot)$ denotes the Hausdorff distance between two curves. The size of K is identical for any point on p. Let $F(\cdot)$ be the position-information vector of a sulcal point in the atlases, which stands for location information in the Euclidean space. Once the size of spherical kernel K is determined, an initial set of neighboring points L_{p_i} within K is obtained as follows:

$$L_{p_i} = \left\{ x \mid x \in s \subseteq S_p, \frac{\|F(x) - F(p_i)\|^2}{r^2} \leq 1 \right\} \ . \tag{4}$$

Our interest is to find sulcal points on the neighboring curves that are "parallel" to curve p, referring to those with similar global shapes and orientations to p. To emphasize such neighboring points in L_{p_i}, we apply the principal component

analysis (PCA) on L_{p_i} since the principal direction u_1 of L_{p_i} stands for the direction of the parallel curves. We then discard as many sulcal points on the neighboring curves as possible that are not parallel to curve p within K, by reducing spherical kernel K to an ellipsoid with its three axes aligned to the three eigenvectors of PCA, $u_n, n = 1, 2, 3$. The eigenvalue λ_1 is given along the first major axis. We then have the following final set of neighboring points L'_{p_i} by letting $l_1 = \sqrt{\lambda_1}$ and $l_2 = l_3 = r$:

$$L'_{p_i} = \left\{ x \mid x \in L_{p_i}, \sum_{n=1}^{3} \frac{((F(x) - F(p_i)) \cdot u_n)^2}{l_n^2} \leq 1 \right\} . \tag{5}$$

Now, we build a bounding cube centered at p_i that fully contains the neighboring sulcal points in L'_{p_i}. Then, we uniformly divide the cube into m subvolumes. Let h_k be a ratio of points in L'_{p_i} that belong to a subvolume b_k, $1 \leq k \leq m$. We finally have a histogram $H_{p_i} = [h_1, h_2, \cdots, h_m]^T$ by the following equation.

$$h_k = \frac{\sum_{x \in L'_{p_i}} I(x, b_k)}{\left| L'_{p_i} \right|} , \tag{6}$$

$$I(x, b_k) = \begin{cases} 1 & \text{if } \{x\} \cap b_k \nsubseteq \emptyset, \\ 0 & \text{otherwise.} \end{cases} \tag{7}$$

For a sulcal point q_j in the subject, it is difficult to compute its actual spherical kernel because its neighboring major curves are unknown. Therefore, for an assignment $a = (p_i, q_j)$, we use the same kernel as p_i in the atlas for computing the histogram of q_j.

Synchronized Curve Matching. To account for sulcal shape variability, we generate the mean curve for each major curve [5]. We denote $\phi(\cdot)$ as the corresponding point on the mean curve to a given sulcal point in the atlas. For an assignment $a = (p_i, q_j)$, we now set a threshold of the distance between p_i and q_j with respect to the covariance of $\phi(p_i)$. Thus, the assignment a is rejected if

$$\sum_{n=1}^{3} \frac{((F(q_j) - F(p_i)) \cdot v_n)^2}{(3\tau_n)^2} > 1 , \tag{8}$$

where $\tau_n^2 (n = 1, 2, 3)$ are the covariances along the corresponding principal axes of the covariance matrix of $\phi(p_i)$. This constrains assignments statistically valid in terms of the sulcal shape variability.

Let s be a neighboring curve for a given major curve p as we defined above. We first measure affinities for p and s, respectively. To incorporate affinities of the neighboring curves into the affinity matrix M, we also measure all possible pairwise affinities between p and s. For $p_i \in p$ and $s_{i'} \in s$, suppose that assignments are given by $a = (p_i, q_j)$ and $b = (s_{i'}, q_{j'})$, where q_j, $q_{j'} \in q \subseteq Q$. Since a major curve is unable to share an identical label with its neighboring curves,

in such a undesirable case of the coexistence of a and b, the pairwise affinity between a and b is set to zero. Once M is built, we compute the principal eigenvector of M to find the highly confident assignments. Since s only helps find the correspondences between p and q, the possibly remaining assignments in s will be left out.

2.2 Joint Labeling Using Multiple Atlases

It is worth noting that major curves in the atlases could be only partially similar to those in the subject. For all major sulcal curves in P, once the highly confident assignments with the corresponding curves in Q are selected, we incorporate the assignments to determine final labels based on their correspondences. Let p^α and p^β be the distinct major sulcal curves in P with an identical label. For two distinct assignments $a = (p_i^\alpha, q_j)$ and $b = (p_{i'}^\beta, q_{j'})$, it is highly desirable that $q_j = q_{j'}$ if $\phi(p_i^\alpha) = \phi(p_{i'}^\beta)$. To implement that idea, we construct a new affinity matrix M that describes relationships of all possible assignments between p^α and p^β. The diagonal entries of M are filled with confidence values that are obtained from the principal eigenvector of the affinity matrix in Sect. 2.1. For two distinct assignments $a = (p_i^\alpha, q_j)$ and $b = (p_{i'}^\beta, q_{j'})$, $M(a, b)$ is set to $A(a, b)$ as defined in Eq. 2. Then, $M(a, b)$ is updated as follows by letting $c = (q_j, q_{j'})$ if $\phi(p_i^\alpha) = \phi(p_{i'}^\beta)$:

$$M(a, b) = A(a, b) \cdot A(c) \; . \tag{9}$$

Finally, we compute the principal eigenvector of M to select the highly confident assignments for the joint labeling.

3 Experimental Results

Since the dataset in [5] is not publicly available, we used the MRIs Surfaces Curves dataset [8] for validation (total 12 subjects). However, in this dataset, several major curves delineated by experts were still crossed gyral regions, which slightly differ from the automatically extracted curves we used in the experiment. Thus, we generated ground-truth curves by combining the manual delineation results with the automatically extracted sulcal curves.

Given an automatically labeled curve q and its corresponding ground-truth curve q_g, the labeling accuracy $acc(q, q_g)$ and false positive labeling error $err(q, q_g)$ were measured by the following equations:

$$acc(q, q_g) = \frac{l(q \cap q_g)}{l(q_g)} \text{ and } err(q, q_g) = \frac{l(q - q_g)}{l(q_g)} \; , \tag{10}$$

where $l(\cdot)$ denotes the length of a curve.

In our experiment, we adapted a jackknife technique to validate the accuracy and false positive errors: For each validation set, one subject was leaved out from the subject set to be labeled, and other subjects were regarded as the atlases.

Table 1. 12 Major curves and their neighboring curves

Curve	Neighbors	Curve	Neighbors	Curve	Neighbors	Curve	Neighbors
STS	ITS	ITS	STS, OTS	CS	preCS, postCS	preCS	CS
postCS	CS	SFS	IFS	IFS	SFS	CingS	-
CalcS	colS	OcPS	-	OTS	ITS, colS	colS	OTS, CalcS

12 out of major curves for both left and right hemispheres were used for validation: the superior temporal sulcus (STS), inferior temporal sulcus (ITS), central sulcus (CS), precentral sulcus (preCS), postcentral sulcus (postCS), superior frontal sulcus (SFS), inferior frontal sulcus (IFS), cingulate sulcus (CingS), calcarine sulcus (CalcS), occipito parietal sulcus (OcPS), occipito temporal sulcus (OTS), and collateral sulcus (colS). We selected the neighboring curves for each major sulcal curve based on neuroanatomical prior knowledge as summarized in Table 1. For fair comparison of different methods in all experiments, we used the same set of the deformed atlases obtained by the same registration method [7], even for the conventional method.

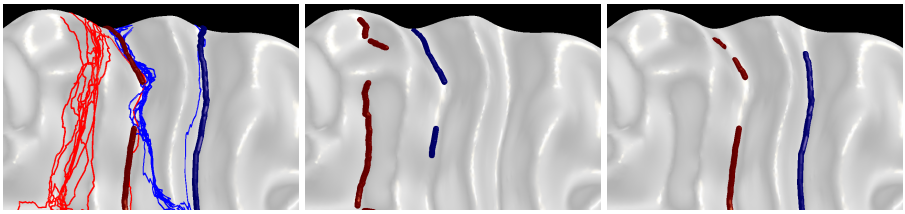

(a) (b) (c)

Fig. 1. Poorly deformed atlases and labeling results for the central sulcus (blue) and postcentral sulcus (red): (a) deformed atlases (thin curves) and the ground-truth curves (bold curves), (b) the labeling results by the conventional method, and (c) the labeling results with neighboring curves

3.1 Neighboring Curves

We employed neighboring curves and chose the most similar curve among multiple atlases for the final result. For the histogram computation, we subdivided the bounding cube into $4 \times 4 \times 4$ subvolumes, i.e., $m = 64$. For the affinity matrix computation, we set the weight vector $w = [0.75, 0.15, 0.05, 0.05]^T$ and the regularization parameter $\sigma = 0.3$. Each of the elements in w corresponds to weight of the position, curvature, tangent vector, and histogram of neighboring sulcal points, respectively. We rejected an assignment if the norm of the difference between the two histograms is greater than 0.1. Note that the parameters were empirically set according to [5] and by our experiment. In Fig. 1, the labeling results with neighboring curves are consistent although the atlases are poorly deformed. The results with neighboring curves exhibited better agreement

Table 2. Average labeling accuracy and false positive errors in the left (lh) and right hemispheres (rh) (unit: %):

	Conventional method		Neighboring curves (a)		Joint labeling (b)		Our method (a+b)	
	lh	rh	lh	rh	lh	rh	lh	rh
Accuracy	68.65	69.19	71.22	72.27	74.53	74.87	77.12	76.47
False positives	20.22	19.85	25.06	23.41	16.82	15.53	15.79	15.46

with the ground-truth than the conventional spectral-based method as summarized in Table 2. Interestingly, the average false positive errors also increased because several false positive assignments that had a low confidence value in the conventional method can gain a higher confidence, resulting from guidance of neighboring curves.

3.2 Joint Labeling Using Multiple Atlases

We applied the joint labeling without guidance of neighboring curves. The results obtained from 12 atlases were incorporated to determine the final label to each major sulcal curve. The same parameter setting as in Sect. 3.1 was used here. Figure 2 shows that the the joint labeling also gives labels to a part of major sulcal curves that is missed in the conventional spectral-based method. Compared to the conventional method, the labeling accuracy increased while the false positive errors decreased as summarized in Table 2.

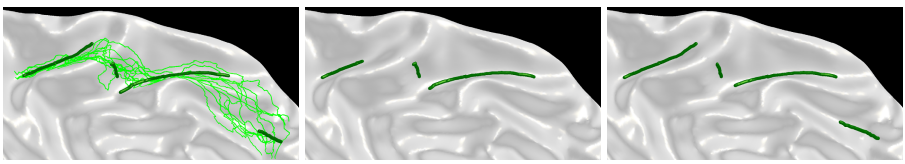

(a) (b) (c)

Fig. 2. Comparison of results by the conventional spectral-based method and joint labeling for the superior frontal sulcus: (a) deformed atlases (thin curves) and the ground-truth curves (bold curves), (b) the labeling results by the conventional spectral-based method, and (c) the labeling results by the joint labeling

3.3 Overall Performance

By incorporating two aspects, i.e., synchronized matching with neighboring curves and joint labeling using multiple atlases, into the our framework, we obtained the overall labeling accuracy and false positive errors as summarized in Table 2.

The labeling performance by our method was highly achieved after incorporating the two aspects. Also, our labeling results were comparable to the corresponding ground-truth curves (see an example in Fig. 3). Figure 4 demonstrates the statistical comparison of the labeling results for 12 major sulcal curves. The results show the average accuracy and false positive errors across subjects. This indicates that our labeling results were consistent on most of the curves, compared to the conventional method.

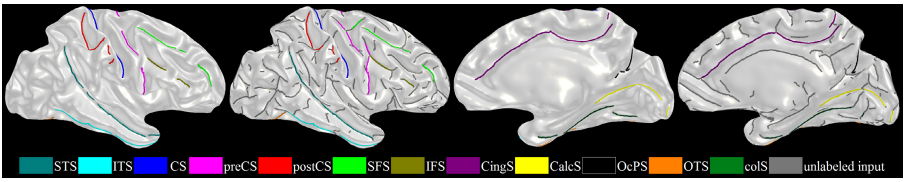

Fig. 3. A visual comparison of our automatic labeling results with the ground-truth for the right hemisphere: the lateral and medial views of ground-truth labeled curves (1st and 3rd columns) and the respective views of automatically labeled curves by our method (2nd and 4th columns). Note that there are many extraneous minor curves in the input (gray). For better visualization, a partially inflated surface model is used.

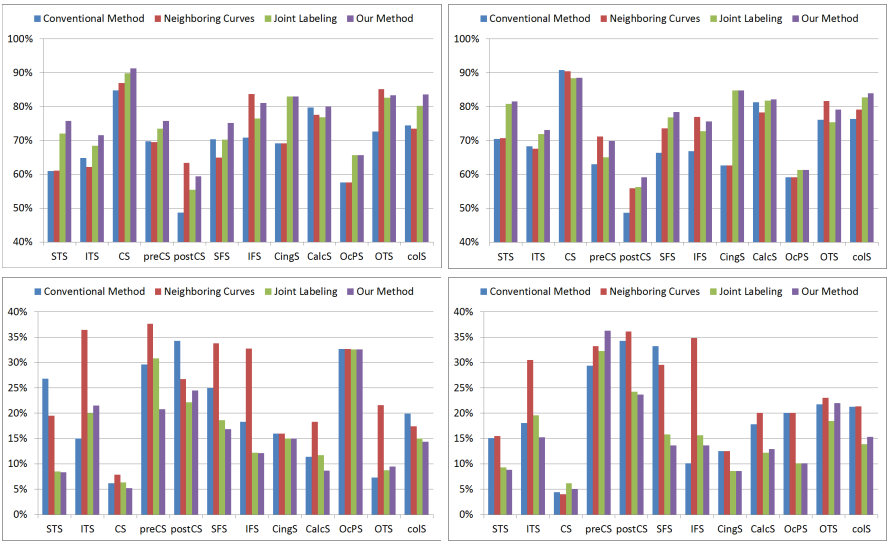

(a) left hemispheres (b) right hemispheres

Fig. 4. Performance comparisons: average labeling accuracy (top row) and false positive errors (bottom row) for major sulcal curves in the left and right hemispheres

4 Conclusion

We presented a method for multiple atlases-based labeling of major sulcal curves on the cortical surface. Specifically, to resolve ambiguity in the labeling, we proposed a histogram feature for each sulcal point and incorporated the geometric information of neighboring curves into the affinity matrix for the curve matching. Since major curves in the atlases are likely to be partially similar to those in the subject, we incorporated the results obtained from all atlases into the linear system for accurate labeling. We have shown in experiment that compared to the conventional method, the performances were improved for 7.87% labeling accuracy and reduced for 4.41% of false positive errors. In our future work, we will employ a learning technique for optimizing parameters used in the curve matching.

References

1. Li, G., Guo, L., Nie, J., Liu, T.: An automated pipeline for cortical sulcal fundi extraction. Medical Image Analysis 14, 343–359 (2010)
2. Seong, J., Im, K., Yoo, S., Seo, S., Na, D., Lee, J.: Automatic extraction of sulcal lines on cortical surfaces based on anisotropic geodesic distance. Neuroimage 49, 293–302 (2010)
3. Lohmann, G., Von Cramon, D.: Automatic labelling of the human cortical surface using sulcal basins. Medical Image Analysis 4, 179–188 (2000)
4. Tao, X., Prince, J., Davatzikos, C.: Using a statistical shape model to extract sulcal curves on the outer cortex of the human brain. IEEE Trans. on Medical Imaging 21, 513–524 (2002)
5. Lyu, I., Seong, J., Shin, S., Im, K., Roh, J., Kim, M., Kim, G., Kim, J., Evans, A., Na, D., et al.: Spectral-based automatic labeling and refining of human cortical sulcal curves using expert-provided examples. Neuroimage 52, 142–157 (2010)
6. Leordeanu, M., Hebert, M.: A spectral technique for correspondence problems using pairwise constraints. In: Computer Vision, ICCV 2005, vol. 2, pp. 1482–1489. IEEE (2005)
7. Yeo, B., Sabuncu, M., Vercauteren, T., Ayache, N., Fischl, B., Golland, P.: Spherical demons: Fast diffeomorphic landmark-free surface registration. IEEE Trans. on Medical Imaging 29, 650–668 (2010)
8. Pantazis, D., Joshi, A., Jiang, J., Shattuck, D., Bernstein, L., Damasio, H., Leahy, R.: Comparison of landmark-based and automatic methods for cortical surface registration. Neuroimage 49, 2479–2493 (2010)